JHEP

Published for SISSA by Springer

Received: April 23, 2014
Revised: June 3, 2014
Accepted: June 17, 2014
Published: July 23, 2014

Fundamental composite Higgs dynamics on the lattice: SU(2) with two flavors

Ari Hietanen,[a] **Randy Lewis,**[b] **Claudio Pica**[a] **and Francesco Sannino**[a]

[a] CP^3-Origins *&* the Danish IAS, *University of Southern Denmark, Campusvej 55, DK-5230 Odense M, Denmark*

[b] *Department of Physics and Astronomy, York University, Toronto, M3J 1P3, Canada*

E-mail: hietanen@cp3-origins.net, randy.lewis@yorku.ca, pica@cp3-origins.net, sannino@cp3-origins.net

Abstract: In reference [1] a unified description, both at the effective and fundamental Lagrangian level, of models of composite Higgs dynamics was proposed. In the unified framework the Higgs itself can emerge, depending on the way the electroweak symmetry is embedded, either as a pseudo-Goldstone boson or as a massive excitation of the condensate. The most minimal fundamental description consists of an SU(2) gauge theory with two Dirac fermions transforming according to the defining representation of the gauge group. We therefore provide first principle lattice results for the massive spectrum of this theory. We confirm the chiral symmetry breaking phenomenon and determine the lightest spin-one axial and vector masses. The knowledge of the energy scale at which new states will appear at the Large Hadron Collider is of the utmost relevance to guide experimental searches of new physics.

Keywords: Lattice Gauge Field Theories, Lattice QCD, Beyond Standard Model, Technicolor and Composite Models

ArXiv ePrint: 1404.2794

doi:10.1007/JHEP07(2014)116

JHEP07(2014)116

Contents

JHEP07(2014)116

1 Introduction

The Standard Model (SM) of particle interactions successfully describes Nature. However, the SM is unappealing. For example the SM Higgs sector simply models spontaneous symmetry breaking, it does not explain it. Furthermore, there is no consistent way to protect the electroweak scale from higher scales, leading to the SM naturalness problem. We refer to [2] for a mathematical classification of different degrees of naturality.

It is well known that by replacing the SM Higgs sector with a fundamental gauge dynamics featuring fermionic matter fields renders the SM Higgs sector natural. Technicolor [3, 4] is a time-honored incarnation of this idea. The Technicolor Higgs [7–11] is the lightest scalar excitation of the fermion condensate responsible for electroweak symmetry breaking. The interplay between the gauge sector and the SM fermion mass sector is relevant because it can reduce the physical mass of the Technicolor Higgs [12]. Other ways to use fundamental dynamics to replace the SM Higgs sector appeared later in [5, 6]. If the underlying dynamics has a larger global symmetry group than the one strictly needed to break the electroweak symmetry successfully, one may be able to choose an electroweak embedding in a way that the electroweak symmetry remains intact. Differently from the Technicolor case, here the Higgs state could be identified with one of the Goldstone Bosons (GB) of the theory. In this case the challenges are not only to provide masses to the SM fermions but also to break the electroweak symmetry by means of yet another sector which can also contribute to give mass to the would-be pseudo-GB Higgs.

In reference [1] a first unified description of models of electroweak composite dynamics was put forward. The description clarified the main similarities, interplay, and shortcomings of Technicolor and composite Goldstone Higgs models. In addition a specific underlying realization in terms of fundamental strongly coupled gauge theories was investigated with a clear link to first principle lattice simulations. It was also shown that for a generic electroweak vacuum alignment, the observed Higgs is neither a purely pGB state nor the Technicolor Higgs, but a mixed state. This result has relevant implications for its physical properties and associated phenomenology.

Given a possible underlying gauge theory featuring fermionic matter one can imagine distinct patterns of chiral symmetry breaking [13–19]. First principle lattice simulations are now in a position to answer these questions [20–33].

The classification of underlying gauge theories relevant for Technicolor models appeared in [17], while for composite models of the Higgs as a pGB can be found in [34, 35]. In reference [1] it was concluded that from the point of view of a fundamental theory with fermionic matter, the minimal scenario to investigate for having both a minimal Technicolor and composite GB Higgs model is based on the global symetry breaking pattern SU(4)→Sp(4), which is locally isomorphic to SO(6)→SO(5). This pattern of chiral symmetry breaking can be achieved dynamically via an underlying SU(2)=Sp(2) gauge theory with 2 Dirac flavors (i.e. four Weyl fermions) transforming according to the fundamental representation of the gauge group. The difference between the Technicolor and the composite pGB Higgs realization lies in the way one embeds the electroweak theory within the global flavor symmetry.

We refer the interested reader to [1] for a detailed description of a phenomenologically viable extension of the Standard Model based on this minimal scenario.

Here we provide state-of-the-art lattice results for the underlying SU(2) gauge theory with 2 Dirac flavors confirming the breaking of the global SU(4) symmetry to Sp(4), first observed in [29], via the formation of a non-perturbative fermion condensate, and in addition we further determine the spin-one spectrum, which is directly relevant for experimental searches of Beyond SM physics.

The paper is organized as follows: in section 2 we introduce the lattice framework and detail how the lattice computations of the spectrum are performed; in section 3 the numerical results are summarised; finally we offer our conclusions in section 4.

2 The lattice method

In the continuum, the Lagrangian for our technicolor template is

$$\mathcal{L} = -\frac{1}{4}F^a_{\mu\nu}F^{a\mu\nu} + \overline{u}(i\gamma^\mu D_\mu - m_u)u + \overline{d}(i\gamma^\mu D_\mu - m_d)d \tag{2.1}$$

which can be discretized in the familiar way to arrive at a Wilson action,

$$\begin{aligned} S_W = & \frac{\beta}{2}\sum_{x,\mu,\nu}\left(1 - \frac{1}{2}\mathrm{ReTr}U_\mu(x)U_\nu(x+\hat{\mu})U^\dagger_\mu(x+\hat{\nu})U^\dagger_\nu(x)\right) + \sum_x \overline{\psi}(x)(4+m_0)\psi(x) \\ & -\frac{1}{2}\sum_{x,\mu}\left(\overline{\psi}(x)(1-\gamma_\mu)U_\mu(x)\psi(x+\hat{\mu}) + \overline{\psi}(x+\hat{\mu})(1+\gamma_\mu)U^\dagger_\mu(x)\psi(x)\right), \end{aligned} \tag{2.2}$$

where U_μ is the gauge field and β the gauge coupling in conventional lattice notation. ψ is the doublet of u and d fermions, and m_0 is the 2×2 diagonal mass matrix.

Mesons will couple to local operators of the form

$$\mathcal{O}^{(\Gamma)}_{\overline{u}d}(x) = \overline{u}(x)\Gamma d(x)\,, \tag{2.3}$$

$$\mathcal{O}^{(\Gamma)}_{\overline{d}u}(x) = \overline{d}(x)\Gamma u(x)\,, \tag{2.4}$$

$$\mathcal{O}^{(\Gamma)}_{\overline{u}u\pm\overline{d}d}(x) = \frac{1}{\sqrt{2}}\left(\overline{u}(x)\Gamma u(x) \pm \overline{d}(x)\Gamma d(x)\right), \tag{2.5}$$

JHEP07(2014)116

where Γ denotes any product of Dirac matrices. Baryons (which are diquarks in this two-color theory) will couple to local operators of the form

$$\mathcal{O}^{(\Gamma)}_{ud}(x) = u^T(x)(-i\sigma^2)C\Gamma d(x)\,, \tag{2.6}$$

$$\mathcal{O}^{(\Gamma)}_{du}(x) = d^T(x)(-i\sigma^2)C\Gamma u(x)\,, \tag{2.7}$$

$$\mathcal{O}^{(\Gamma)}_{uu\pm dd}(x) = \frac{1}{\sqrt{2}}\Big(u^T(x)(-i\sigma^2)C\Gamma u(x) \pm d^T(x)(-i\sigma^2)C\Gamma d(x)\Big)\,, \tag{2.8}$$

where the Pauli structure $-i\sigma^2$ acts on color indices while the charge conjugation operator C acts on Dirac indices.

We extract the meson masses from the two-point correlation functions

$$\begin{aligned} C^{(\Gamma)}_{\overline{u}d}(t_i - t_f) &= \sum_{\vec{x}_i,\vec{x}_f} \Big\langle \mathcal{O}^{(\Gamma)}_{ud}(x_f)\mathcal{O}^{(\Gamma)\dagger}_{ud}(x_i)\Big\rangle\,. \\ &= \sum_{\vec{x}_i,\vec{x}_f} \mathrm{Tr}\,\Gamma S_{d\overline{d}}(x_f,x_i)\gamma^0\Gamma^\dagger\gamma^0 S_{u\overline{u}}(x_i,x_f), \end{aligned} \tag{2.9}$$

where $S_{u\overline{u}}(x,y) = \langle u(x)\overline{u}(y)\rangle$. The quantities of interest are pseudoscalar $\Gamma = \gamma_5$, vector $\Gamma = \gamma_k$ $(k = 1,2,3)$, and axial vector $\Gamma = \gamma_5\gamma_k$ mesons. As a source vector we use $Z_2 \times Z_2$ single time slice stochastic sources [36].

In addition to the meson spectrum we are interested in two other quantities, the quark mass m_{q} and the Goldstone boson decay constant f_Π. We define the quark mass through the Partially Conserved Axial Current (PCAC) relation:

$$m_{\mathrm{q}} = \lim_{t\to\infty} \frac{1}{2}\frac{\partial_t V_\Pi}{V_{\mathrm{PP}}}, \tag{2.10}$$

where

$$\begin{aligned} V_\Pi(t_i - t_f) &= a^3 \sum_{x_1,x_2,x_3} \langle \overline{u}(t_i)\gamma_0\gamma_5 d(t_i)\overline{u}(t_f)\gamma_5 d(t_f)\rangle\ , \\ V_{\mathrm{PP}}(t_i - t_f) &= a^3 \sum_{x_1,x_2,x_3} \langle \overline{u}(t_i)\gamma_5 d(t_i)\overline{u}(t_f)\gamma_5 d(t_f)\rangle\ . \end{aligned} \tag{2.11}$$

The Goldstone boson decay constant can be calculated as:

$$f_\Pi = \frac{2m_{\mathrm{q}}}{m_\Pi^2} G_\Pi, \tag{2.12}$$

where G_Π is obtained from the asymptotic form of V_{PP} at large $t_i - t_f$:

$$V_{\mathrm{PP}}(t_i - t_f) \sim -\frac{G_\Pi^2}{m_\Pi}\exp\left[-m_\Pi(t_i - t_f)\right]. \tag{2.13}$$

To convert the lattice quantities to physical units, one should determine the lattice spacing for our simulations and the appropriate (mass-independent) renormalization constant. The lattice spacing, in a Technicolor model, is fixed by the requirement that the (renormalized) Goldstone boson decay constant has the value of 246 GeV, giving the correct

JHEP07(2014)116

β	Volume	m_0	Therm.	Conf.
2.0	$16^3 \times 32$	-0.85, -0.9, -0.94, -0.945, -0.947, -0.949	320	680
2.0	32^4	-0.947	500	680
2.2	$16^3 \times 32$	-0.60, -0.65, -0.68, -0.70, -0.72, -0.75	320	680
2.2	$24^3 \times 32$	-0.75	500	∼2000
2.2	32^4	-0.72,-0.735, -0.75	500	∼2000

Table 1. Parameters used in the simulations. The thermalization column refers to the number of discarded initial configurations and the configuration column refers to the number of configurations used in measurements.

mass to the electroweak gauge bosons. For the general composite Higgs scenario the electroweak decay constant becomes $\sin(\theta)\, f_\Pi$ with the θ depending on the specific electroweak embedding. The actual value of θ depends on the electroweak quantum corrections, the top corrections as well as the effects of other possible sources of explicit breaking of the initial SU(4) symmetry. The Technicolor limit is recovered for $\theta = \pi/2$ while the composite pGB Higgs case corresponds to small, but non-vanishing, θ. Any other value of the θ is allowed and corresponds to a combination of these two limits. For the details we refer to [1]. For definitiveness we present the results for $\sin(\theta) = 1$ but we will reinstate the dependence on θ for the spectrum.

The relevant renormalization constant for f_Π, commonly denoted in the literature by Z_a, has not been computed non-perturbatively for our simulations. In this work we use the perturbative value which has been calculated in [22]. For fermions in the fundamental representation we have:

$$Z_a = 1 - \frac{g_0^2}{16\pi^2}\frac{N^2-1}{2N}15.7 \stackrel{N=2}{=} 1 - 0.2983/\beta. \tag{2.14}$$

3 The lattice results

The lattice simulations used in this work extend the results already published in ref. [29]. In particular, we have used larger volumes for the set of parameters closest to the chiral limit. The bare parameters used for our simulations are listed in table 1, where we also report the number of thermalized configurations, of length one, used in our analysis below. Thermalizations are estimated by monitoring the average plaquette expectation value and the value of the two-point correlation function in the pseudoscalar channel at a time separation of twelve time slices. These two quantities are shown in figure 1 for two representative light quark masses on the finest lattices used in this work.

All the ensembles of gauge configurations were created using the GPU version of the HiRep code [23]. The lattice action used is the plaquette-action SU(2) gauge theory with two flavors (u and d) of mass-degenerate Wilson fermions. The Hybrid Monte Carlo trajectory length was chosen to be one. The autocorrelation times for plaquette expectation values and meson correlators were estimated to be about 10. The errors for all quantities extracted in this work were obtained using a bootstrap procedure.

JHEP07(2014)116

β	Volume	m_0	m_q	m_Π	m_ρ	m_A	f_Π
2.0	32×16^3	-0.85	0.1919(6)	0.9163(18)	1.008(20)	1.64(3)	0.1544(4)
2.0	32×16^3	-0.9	0.1134(6)	0.708(3)	0.821(3)	1.47(3)	0.1248(5)
2.0	32×16^3	-0.94	0.0476(8)	0.451(7)	0.636(5)	1.15(4)	0.089(9)
2.0	32×16^3	-0.945	0.038(7)	0.407(5)	0.57(6)	1.08(3)	0.0799(7)
2.0	32×16^3	-0.947	0.0327(7)	0.377(6)	0.546(7)	1.02(4)	0.0754(8)
2.0	32×16^3	-0.949	0.0307(8)	0.374(6)	0.546(9)	1.02(3)	0.075(12)
2.0	32^4	-0.947	0.0309(3)	0.3739(14)	0.536(4)	1.0(5)	0.0766(6)
2.2	32×16^3	-0.6	0.2296(7)	0.886(3)	0.93(3)	1.371(12)	0.1119(5)
2.2	32×16^3	-0.65	0.1637(7)	0.755(3)	0.792(3)	1.229(9)	0.0992(5)
2.2	32×16^3	-0.68	0.1205(7)	0.612(4)	0.671(5)	1.068(17)	0.0868(5)
2.2	32×16^3	-0.7	0.0968(7)	0.548(5)	0.615(6)	1.018(12)	0.0793(5)
2.2	32×16^3	-0.72	0.0686(6)	0.455(5)	0.531(5)	0.884(19)	0.0684(5)
2.2	32×16^3	-0.75	0.0264(8)	0.324(8)	0.445(9)	0.76(3)	0.0405(12)
2.2	32×24^3	-0.75	0.024(5)	0.258(4)	0.359(8)	0.62(4)	0.0433(9)
2.2	32^4	-0.72	0.0661(5)	0.4475(8)	0.522(14)	0.81(3)	0.0664(5)
2.2	32^4	-0.735	0.0456(3)	0.3612(18)	0.446(4)	0.75(3)	0.0568(5)
2.2	32^4	-0.75	0.0257(5)	0.2649(16)	0.363(5)	0.59(6)	0.0457(7)

Table 2. The values obtained in simulations for PCAC-quark mass, Goldstone boson mass, vector meson mass, axial vector meson mass, and Goldstone boson decay constant as function of β, volume and bare quark mass.

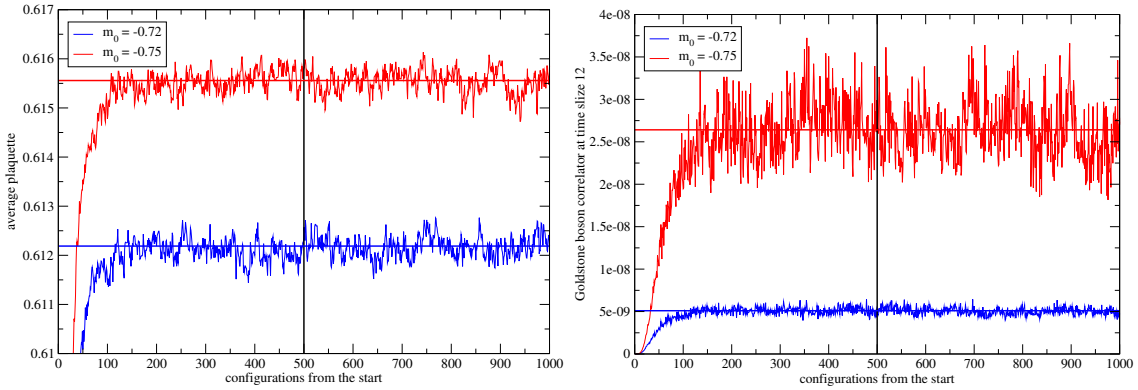

Figure 1. Left: the first 1000 measurements of average plaquette. Right: the first 1000 measurements of the Goldstone boson correlator at time slice 12. The simulations were performed with volume $V = 32^4$ and coupling $\beta = 2.2$. The configurations left of black vertical line are discarded as unthermalized.

In a previous work by some of the authors [29], a first estimate of the Goldstone spectrum was already obtained. However large finite volume effects were observed — see figure 5(b) of [29] — for the lightest value of the quark mass on the finest lattice used in that work, corresponding to the bare parameter couplings $(\beta, m_0) = (2.2, -0.75)$.

Here we perform a more systematic analysis to control finite volume effects, using simulations on three different lattice volumes $V = 32 \times 16^3$, 32×24^3, and 32^4 at the

JHEP07(2014)116

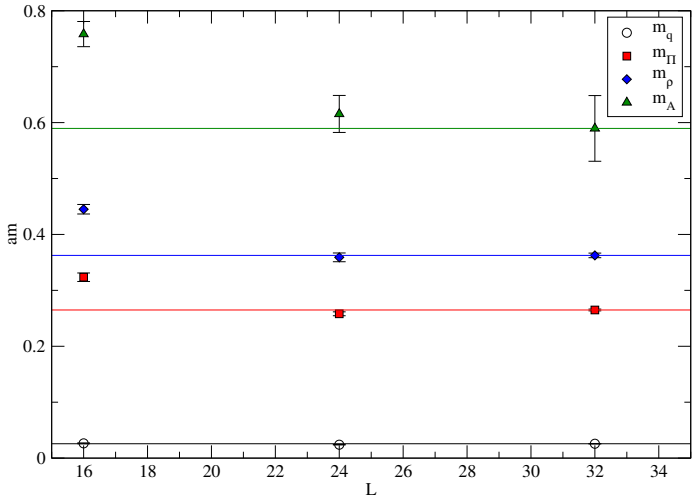

Figure 2. The PCAC quark mass, Goldstone boson, vector meson, and axial vector meson mass as a function of lattice size L, on the most chiral point $m_0 = -0.75$ and $\beta = 2.2$. The measurements on two larger lattices are inside statistical errors.

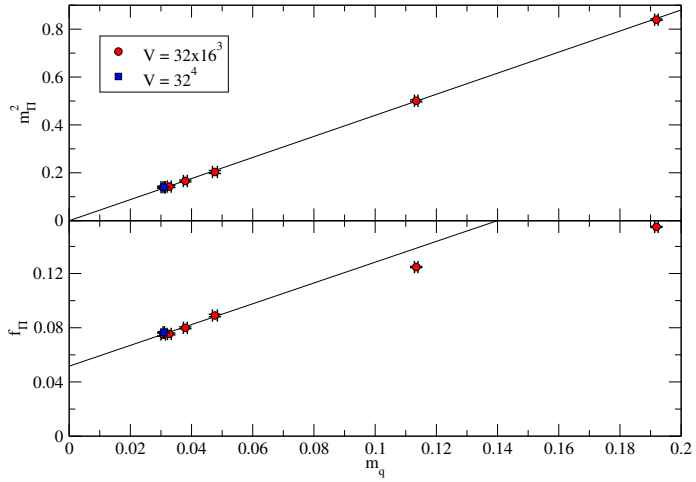

Figure 3. The Goldstone boson mass squared and its decay constant as a function of the quark mass for $\beta = 2.0$. Extrapolations to the chiral limit, as discussed in the text, are also shown.

lightest quark mass on the finest lattice. At this quark mass, the results for the smallest volume 32×16^3 suffer clearly from finite volume effects, whereas observables measured on the two largest lattices agree within statistical errors, as shown in figure 2. From the size of the statistical errors on the two largest lattices, we estimate that the residual finite volume effects at our lightest quark mass are below 2% for m_Π, f_Π and m_ρ and below 10% for m_A.

To confirm spontaneous chiral symmetry breaking one should, in principle, reach the chiral regime of the theory, pushing the quark masses light enough that chiral perturbation theory (χPT), or the appropriate lattice extension of it, could be used, while keeping under control all other systematic sources of error which are present on the lattice. It is well known, by studies of QCD, that this chiral regime is extremely difficult to reach as

JHEP07(2014)116

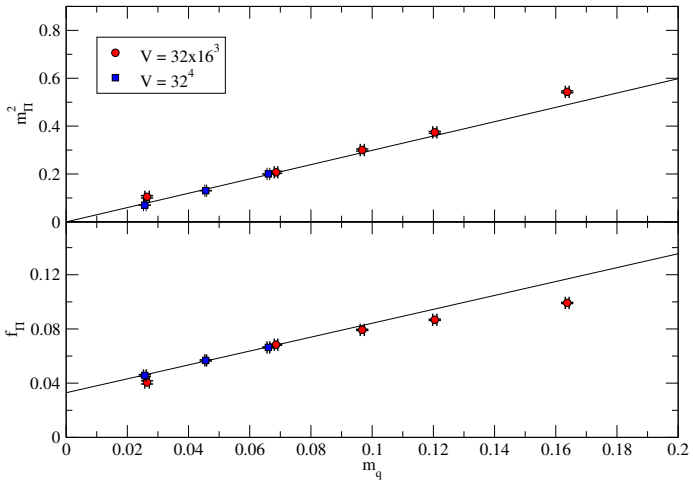

Figure 4. The Goldstone boson mass squared and its decay constant as a function of the quark mass for $\beta = 2.2$. Extrapolations to the chiral limit, as discussed in the text, are also shown.

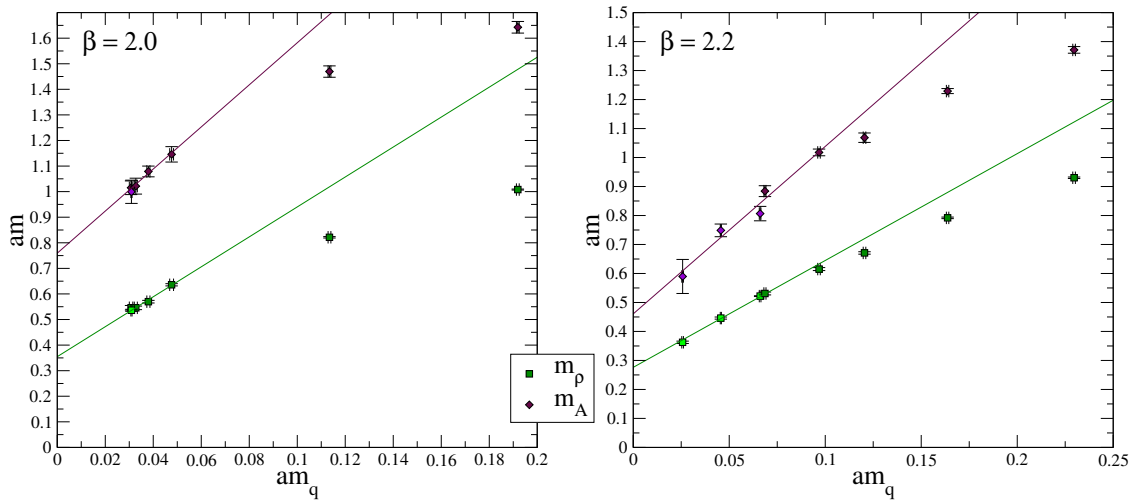

Figure 5. Vector and axial vector meson mass as a function of PCAC quark mass with two different lattice spacings. A linear extrapolation to the chiral limit works well with $m_q < 0.1$.

lattice artifacts and residual finite volume effects tend to make the predictions of χPT difficult to test.

Keeping this in mind, we analyze our data for signs of spontaneous chiral symmetry breaking and check how well predictions from χPT fit the measured Goldstone spectrum. The Goldstone boson mass and decay constant are studied as a function of quark mass, defined through the PCAC relation and compared with the expectations from (continuum) chiral perturbation theory at next to leading order (NLO):

$$\frac{m_{\Pi}^2}{m_{\rm q}} = 2B\left[1 + Cx\log x + Dx + \mathcal{O}(m_{\rm q}^2)\right] \ , \tag{3.1}$$

JHEP07(2014)116

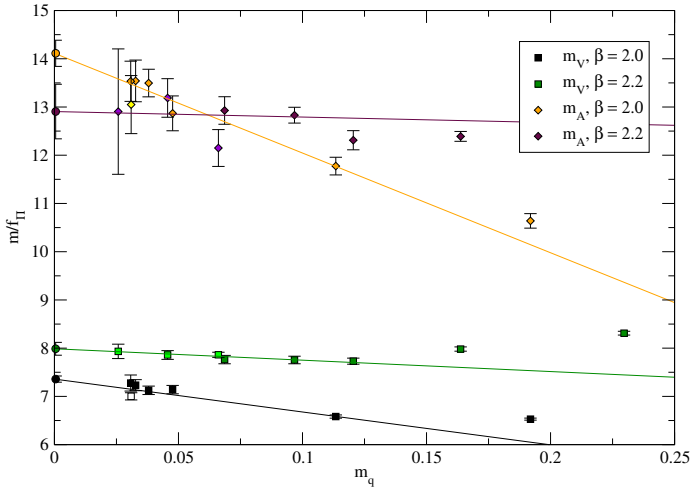

Figure 6. The vector meson and axial vector meson masses in physical units. The chiral extrapolations have been performed using a linear fit to the points where $m_q < 0.12$.

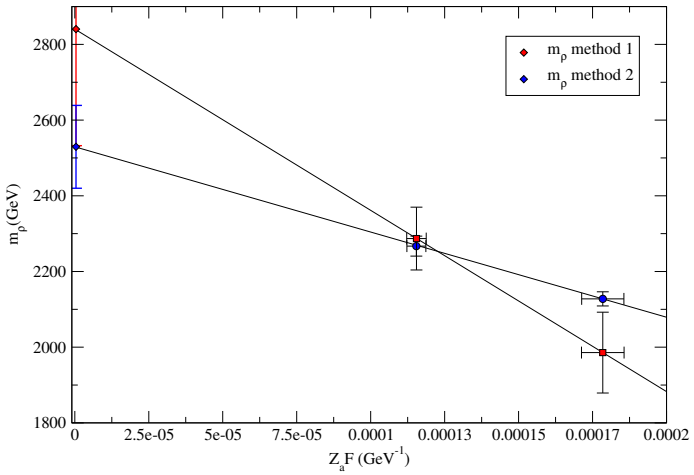

Figure 7. A continuum extrapolation of the vector meson mass.

and

$$f_{\Pi} = F\left[1 + C' x \log x + D' x + \mathcal{O}(m_{\mathrm{q}}^2)\right] \ , \tag{3.2}$$

where B, F, D and D' are (unknown) low-energy constants of the theory, $x \equiv \frac{2Bm_{\mathrm{q}}}{16\pi^2 F^2}$ and C and C' are known constants. For our theory $C = -\frac{1}{2} - \frac{1}{2N_f} = -\frac{3}{4}$ and $C' = \frac{1}{2}N_f = 1$. Additional terms in the chiral expansion can also be computed for the NNLO approximations. The relevant expressions can be found in [37], from which the quoted values for C and C' were taken.

Correction to the continuum chiral expansion arise due to the lattice discretisation at non-zero lattice spacing. For Wilson fermions at NLO the functional form of eqs. (3.1) and (3.2) remains unchanged, but the coefficients, and in particular C and C', depend on the lattice spacing a. In the limit $a \to 0$ one should recover the continuum values for C

JHEP07(2014)116

	β	range	χ^2/dof	dof	LO coefficient
m_Π^2	2.0	$m_q < 0.05$	0.48	2	$B = 4.2(2.3)$
f_Π	2.0	$m_q < 0.05$	2.28	2	$F = 0.13(5)$
m_Π^2	2.2	$m_q < 0.07$	0.32	1	$B = 1.34(16)$
f_Π	2.2	$m_q < 0.07$	2.01	1	$F = 0.028(6)$

Table 3. NLO Wilson χPT fits to our data for m_Π^2 and f_Π. All the fits are acceptable in the quoted quark mass range. The last column "LO coefficient" refers to the coefficients B and F of the chiral expansion for the Goldstone boson mass squared and for its decay constant.

and C', however for a fixed lattice spacing C and C' are two additional free parameters of the expansion.

We show in figures 3 and 4 our results for m_Π^2 and f_Π for the two values of the lattice spacing used in this work. It is possible to use NLO Wilson chiral perturbation theory to fit our data at small quark masses for both m_Π^2 and f_Π. We report in table 3 the quark mass ranges, χ^2 and the coefficients B and F for the fits for the two different values of the lattice spacing used in this work. The relative errors on the fitting parameters are large especially for the coefficients C and C' of the $x \log x$ terms of the chiral expansion which suffer from very large uncertainties $\sim 100\%$, and are thus compatible with zero. This can be explained by our data not being yet in a regime where the $x \log x$ terms can be clearly distinguished from the polynomial terms in the expansion, even at the lightest quark masses available.

Given that the chiral logs are subdominant, a simple polynomial fit to the data is expected to be an adequate description of m_Π^2 and f_Π. We therefore fit our data setting $C = C' = 0$. The values for B and F thus obtained are given in table 4. The central values of B and F are compatible, within statistical errors, with the ones obtained using NLO Wilson chiral perturbation theory. In the analysis below we use these values of B and F as our best estimate, and consider the errors from different fitting procedures as systematic errors. In the last column of table 4, we use the perturbative value of Z_a from eq. (2.14) to obtain the renormalized F.

We also note that our data are not well described by NLO or NNLO continuum chiral perturbation theory, i.e. when the coefficients C and C' of the logarithmic terms are fixed. In this case we can perform a simultaneous fit of both m_Π^2 and f_Π, and the fit is thus much more constrained. The resulting $\chi^2/\text{dof} \sim 100$ shows that this is not a good description of our data.

The values of vector and axial vector meson masses, as measured from our ensemble of configurations, are plotted in figure 5. A linear function represents the data well at small quark masses $m_\text{q} < 0.1$.

Given that f_Π, m_ρ and m_A are well described by a linear function at small quark masses, one can expect that the two ratios m_ρ/f_Π and m_A/f_Π are also linear functions of the quark mass close to the chiral limit. These ratios are shown in figure 6, together with a linear extrapolation to zero quark mass. We will refer to this method of chiral extrapolation as "method 2", whereas the first method will be named "method 1" in the following.

JHEP07(2014)116

β	B	F	Z_a	Z_aF
2.0	2.52(12)	0.052(3)	0.85	0.0439(18)
2.2	1.26(03)	0.033(1)	0.86	0.0285(08)

Table 4. The fitted values for the coefficients B and F of the chiral expansion. The functional form used is a polynomial in the quark mass, as explained in the text. The corresponding χ^2/dof are 0.51 and 3.4 for $\beta = 2.0$, and 0.28 and 1.5 for $\beta = 2.2$ for m_Π^2 and f_Π respectively. In the last column we report the value of the renormalized F obtained using the perturbative value of Z_a.

We use these two different methods as a crosscheck of the chiral extrapolation and to try to quantify the systematic errors due to the choice of extrapolation function. We compare in table 5 the results in lattice units for the chiral extrapolations. The methods are clearly consistent with each other and method 2 leads to an overall smaller statistical error.

Combining the data from the two lattice spacings available in this study, we can perform a first, crude continuum extrapolation for the masses of the vector and axial vector mesons. As explained above, the lattice spacing is fixed by the requirement that the value of the renormalized Goldstone decay constant satisfies $f_\Pi \sin(\theta) = 246$ GeV, as required to give the correct masses to the electroweak gauge bosons. For concreteness here we assume $sin(\theta) = 1$, but the dependence on θ can easily be reinstated when required as done below. The results of the linear extrapolations of $m_\rho/(Z_aF)$ and $m_A/(Z_aF)$ to the continuum limit are reported in table 6.

Our continuum extrapolation is subject to two major sources of systematic errors. First our simulations are performed only at two lattice spacings, and therefore we do not have a good measure of how well our linear extrapolation describes the data. To take this into account, as a systematic error we quote, quite conservatively, the difference between the value of the continuum extrapolated value and the data point of the finer lattice. The second systematic error stems from the renormalization constant Z_a which we do not measure non-perturbatively. As a systematic error we then use the difference between the perturbative value of $Z_a = Z_{\rm a}^{\rm pert}$ and $Z_{\rm a} = 1$. In table 6 we list the continuum extrapolated values of vector and axial vector mesons for both methods 1 and 2 described above for chiral extrapolation. The vector case is plotted in figure 7.

The results produced by both methods are comparable and well inside each other's error bars. As final results for the meson masses we quote the one obtained by method 2. Square summing the errors, the vector meson reads $m_\rho \sin(\theta) = 2.5 \pm 0.5$ TeV and the axial vector meson $m_A \sin(\theta) = 3.3 \pm 0.7$ TeV where we have reinstated the dependence on the angle θ defining the specific electroweak embedding.

From a purely phenomenological point of view in the limit $\theta = \pi/2$ this model goes over to non-walking Technicolor-like theories. Assuming a traditional effective four-fermion way to give masses to the SM fermions (see [11] for a review), a walking theory example can be achieved starting from this model by adding adjoint matter as put forward in [40]. Although we expect the spectrum of the theory to change, the theory investigated here is the (lattice) building block to start exploring the more involved but highly interesting walking version. For any other value of θ we refer to [1] for the different ways one can address fermion mass generation.

JHEP07(2014)116

	β	Method 1	Method 2
$m_\rho/(Z_a F)$	2.0	8.1(5)	8.65(8)
$m_\rho/(Z_a F)$	2.2	9.3(4)	9.22(11)
$m_A/(Z_a F)$	2.0	18(2)	16.6(4)
$m_A/(Z_a F)$	2.2	17(3)	15.5(6)

Table 5. The chiral extrapolated values for the vector and axial vector mesons in units of the renormalized Goldstone boson decay constant. Only the statistical error is reported here.

	β	Method 1 (GeV)	Method 2 (GeV)
m_ρ	∞	2840(330)(560)(360)	2520(100)(240)(310)
m_A	∞	4000(1800)(200)(430)	3300(400)(510)(340)

Table 6. The continuum extrapolated values for the vector and axial vector mesons. The conversion to physical units is done requiring $Z_a F = a \cdot 246$ GeV. The first error is statistical, the second one is the systematic from a linear continuum extrapolation with only two data points, and the third one comes from the uncertainty on Z_a.

Last but not the least it is worth mentioning that light dark matter, in this model, can be achieved only in the Technicolor limit [1]. This work is therefore complementary to the one in [29, 32].

4 Conclusions

The SU(2)-gauge theory with two fundamental fermions unifies both Technicolor and composite pGB Higgs models of electroweak symmetry breaking. In this work, we have calculated the masses of the two lightest non-singlet mesons using the Goldstone boson decay constant to set the scale. We performed the calculations with two different lattice spacings. With conservative error estimates the mass of the lightest vector meson $m_\rho \sin(\theta)$ is 2.5 ± 0.5TeV. This value is clearly above one TeV and outside the current exclusion limits set by the LHC [39].

To increase the precision of our results for the spectrum, at least one additional lattice spacing is required alongside a nonperturbative determination of the renormalization constant Z_a. This would require a significant increase of computational resources. Furthermore we are eager to investigate the scalar sector and the vector decay constants.

Acknowledgments

This work was supported by the Danish National Research Foundation DNRF:90 grant, by a Lundbeck Foundation Fellowship grant, and by NSERC of Canada. The computing facilities were provided by the Danish Centre for Scientific Computing and Canada's Shared Hierarchical Academic Research Computing Network (SHARCNET: http://www.sharcnet.ca).

JHEP07(2014)116

References

[1] G. Cacciapaglia and F. Sannino, *Fundamental Composite (Goldstone) Higgs Dynamics*, arXiv:1402.0233 [INSPIRE].

[2] O. Antipin, M. Mojaza and F. Sannino, *Conformal Extensions of the Standard Model with Veltman Conditions*, *Phys. Rev.* **D 89** (2014) 085015 [arXiv:1310.0957] [INSPIRE].

[3] S. Weinberg, *Implications of Dynamical Symmetry Breaking*, *Phys. Rev.* **D 13** (1976) 974 [INSPIRE].

[4] L. Susskind, *Dynamics of Spontaneous Symmetry Breaking in the Weinberg-Salam Theory*, *Phys. Rev.* **D 20** (1979) 2619 [INSPIRE].

[5] D.B. Kaplan and H. Georgi, $SU(2) \times U(1)$ *Breaking by Vacuum Misalignment*, *Phys. Lett.* **B 136** (1984) 183 [INSPIRE].

[6] D.B. Kaplan, H. Georgi and S. Dimopoulos, *Composite Higgs Scalars*, *Phys. Lett.* **B 136** (1984) 187 [INSPIRE].

[7] F. Sannino and J. Schechter, *Chiral phase transition for* $SU(N)$ *gauge theories via an effective Lagrangian approach*, *Phys. Rev.* **D 60** (1999) 056004 [hep-ph/9903359] [INSPIRE].

[8] D.K. Hong, S.D.H. Hsu and F. Sannino, *Composite Higgs from higher representations*, *Phys. Lett.* **B 597** (2004) 89 [hep-ph/0406200] [INSPIRE].

[9] D.D. Dietrich, F. Sannino and K. Tuominen, *Light composite Higgs from higher representations versus electroweak precision measurements: Predictions for CERN LHC*, *Phys. Rev.* **D 72** (2005) 055001 [hep-ph/0505059] [INSPIRE].

[10] D.D. Dietrich, F. Sannino and K. Tuominen, *Light composite Higgs and precision electroweak measurements on the Z resonance: An Update*, *Phys. Rev.* **D 73** (2006) 037701 [hep-ph/0510217] [INSPIRE].

[11] F. Sannino, *Conformal Dynamics for TeV Physics and Cosmology*, *Acta Phys. Polon.* **B 40** (2009) 3533 [arXiv:0911.0931] [INSPIRE].

[12] R. Foadi, M.T. Frandsen and F. Sannino, *125 GeV Higgs from a not so light Technicolor Scalar*, *Phys. Rev.* **D 87** (2013) 095001 [arXiv:1211.1083] [INSPIRE].

[13] M.E. Peskin, *The Alignment of the Vacuum in Theories of Technicolor*, *Nucl. Phys.* **B 175** (1980) 197 [INSPIRE].

[14] J. Preskill, *Subgroup Alignment in Hypercolor Theories*, *Nucl. Phys.* **B 177** (1981) 21 [INSPIRE].

[15] D.A. Kosower, *Symmetry breaking patterns in pseudoreal and real gauge theories*, *Phys. Lett.* **B 144** (1984) 215 [INSPIRE].

[16] F. Sannino and K. Tuominen, *Orientifold theory dynamics and symmetry breaking*, *Phys. Rev.* **D 71** (2005) 051901 [hep-ph/0405209] [INSPIRE].

JHEP07(2014)116

[17] D.D. Dietrich and F. Sannino, *Conformal window of* SU(N) *gauge theories with fermions in higher dimensional representations*, *Phys. Rev.* **D 75** (2007) 085018 [hep-ph/0611341] [INSPIRE].

[18] F. Sannino, *Conformal Windows of SP(2N) and* SO(N) *Gauge Theories*, *Phys. Rev.* **D 79** (2009) 096007 [arXiv:0902.3494] [INSPIRE].

[19] M. Mojaza, C. Pica, T.A. Ryttov and F. Sannino, *Exceptional and Spinorial Conformal Windows*, *Phys. Rev.* **D 86** (2012) 076012 [arXiv:1206.2652] [INSPIRE].

[20] S. Catterall and F. Sannino, *Minimal walking on the lattice*, *Phys. Rev.* **D 76** (2007) 034504 [arXiv:0705.1664] [INSPIRE].

[21] S. Catterall, J. Giedt, F. Sannino and J. Schneible, *Phase diagram of* SU(2) *with 2 flavors of dynamical adjoint quarks*, *JHEP* **11** (2008) 009 [arXiv:0807.0792] [INSPIRE].

[22] L. Del Debbio, M.T. Frandsen, H. Panagopoulos and F. Sannino, *Higher representations on the lattice: Perturbative studies*, *JHEP* **06** (2008) 007 [arXiv:0802.0891] [INSPIRE].

[23] L. Del Debbio, A. Patella and C. Pica, *Higher representations on the lattice: Numerical simulations.* SU(2) *with adjoint fermions*, *Phys. Rev.* **D 81** (2010) 094503 [arXiv:0805.2058] [INSPIRE].

[24] S. Catterall, J. Giedt, F. Sannino and J. Schneible, *Probes of nearly conformal behavior in lattice simulations of minimal walking technicolor*, arXiv:0910.4387 [INSPIRE].

[25] A.J. Hietanen, K. Rummukainen and K. Tuominen, *Evolution of the coupling constant in* SU(2) *lattice gauge theory with two adjoint fermions*, *Phys. Rev.* **D 80** (2009) 094504 [arXiv:0904.0864] [INSPIRE].

[26] L. Del Debbio, B. Lucini, A. Patella, C. Pica and A. Rago, *Conformal versus confining scenario in* SU(2) *with adjoint fermions*, *Phys. Rev.* **D 80** (2009) 074507 [arXiv:0907.3896] [INSPIRE].

[27] J.B. Kogut and D.K. Sinclair, *Thermodynamics of lattice QCD with 2 flavours of colour-sextet quarks: A model of walking/conformal Technicolor*, *Phys. Rev.* **D 81** (2010) 114507 [arXiv:1002.2988] [INSPIRE].

[28] T. Karavirta, J. Rantaharju, K. Rummukainen and K. Tuominen, *Determining the conformal window:* SU(2) *gauge theory with* $N_f = 4$*, 6 and 10 fermion flavours*, *JHEP* **05** (2012) 003 [arXiv:1111.4104] [INSPIRE].

[29] R. Lewis, C. Pica and F. Sannino, *Light Asymmetric Dark Matter on the Lattice:* SU(2) *Technicolor with Two Fundamental Flavors*, *Phys. Rev.* **D 85** (2012) 014504 [arXiv:1109.3513] [INSPIRE].

[30] A. Hietanen, C. Pica, F. Sannino and U.I. Sondergaard, *Isotriplet Dark Matter on the Lattice:* SO(4)*-gauge theory with two Vector Wilson fermions*, PoS(LATTICE 2012)065 [arXiv:1211.0142] [INSPIRE].

[31] A. Hietanen, C. Pica, F. Sannino and U.I. Sondergaard, *Orthogonal Technicolor with Isotriplet Dark Matter on the Lattice*, *Phys. Rev.* **D 87** (2013) 034508 [arXiv:1211.5021] [INSPIRE].

[32] A. Hietanen, R. Lewis, C. Pica and F. Sannino, *Composite Goldstone Dark Matter: Experimental Predictions from the Lattice*, arXiv:1308.4130 [INSPIRE].

JHEP07(2014)116

[33] A. Hietanen, C. Pica, F. Sannino and U. Søndergaard, *Predictions for LHC from* SO(4) *MWT*, arXiv:1311.3841 [INSPIRE].

[34] J. Mrazek, A. Pomarol, R. Rattazzi, M. Redi, J. Serra et al., *The Other Natural Two Higgs Doublet Model*, *Nucl. Phys.* **B 853** (2011) 1 [arXiv:1105.5403] [INSPIRE].

[35] B. Bellazzini, C. Csáki and J. Serra, *Composite Higgses*, arXiv:1401.2457 [INSPIRE].

[36] P.A. Boyle, A. Juttner, C. Kelly and R.D. Kenway, *Use of stochastic sources for the lattice determination of light quark physics*, *JHEP* **08** (2008) 086 [arXiv:0804.1501] [INSPIRE].

[37] J. Bijnens and J. Lu, *Technicolor and other QCD-like theories at next-to-next-to-leading order*, *JHEP* **11** (2009) 116 [arXiv:0910.5424] [INSPIRE].

[38] J. Gasser and H. Leutwyler, *Chiral Perturbation Theory: Expansions in the Mass of the Strange Quark*, *Nucl. Phys.* **B 250** (1985) 465 [INSPIRE].

[39] ATLAS collaboration, *Search for high-mass resonances decaying to dilepton final states in pp collisions at* $s^{1/2} = 7$*-TeV with the ATLAS detector*, *JHEP* **11** (2012) 138 [arXiv:1209.2535] [INSPIRE].

[40] T.A. Ryttov and F. Sannino, *Ultra Minimal Technicolor and its Dark Matter TIMP*, *Phys. Rev.* **D 78** (2008) 115010 [arXiv:0809.0713] [INSPIRE].

JHEP07(2014)116